Specific heat studies of pure Nb_3Sn single crystals at low temperature

2009 J. Phys.: Condens. Matter 21 325701

(http://iopscience.iop.org/0953-8984/21/32/325701)

IOP PUBLISHING JOURNAL OF PHYSICS: CONDENSED MATTER

J. Phys.: Condens. Matter **21** (2009) 325701 (7pp) doi:10.1088/0953-8984/21/32/325701

Specific heat studies of pure Nb_3Sn single crystals at low temperature

R Escudero[1,3], F Morales[1] and S Bernès[2]

[1] Instituto de Investigaciones en Materiales, Universidad Nacional Autónoma de México, Apartado Postal 70-360, México, DF 04510, Mexico
[2] Facultad de Ciencias Químicas, Universidad Autónoma de Nuevo León, Monterrey Nuevo León, Mexico

E-mail: escu@servidor.unam.mx

Received 29 April 2009, in final form 11 June 2009
Published 13 July 2009
Online at stacks.iop.org/JPhysCM/21/325701

Abstract

Specific heat measurements performed on high purity vapor-grown Nb_3Sn crystals show clear features related to both the martensitic and superconducting transitions. Our measurements indicate that the martensitic anomaly does not display hysteresis, meaning that the martensitic transition could be a weak first-order or a second-order thermodynamic transition. Careful measurements of the two transition temperatures display an inverse correlation between them. At low temperature, specific heat measurements show the existence of a single superconducting energy gap feature.

(Some figures in this article are in colour only in the electronic version)

1. Introduction

Nb_3Sn is a well known intermetallic compound with a cubic A15 structure at room temperature. It displays two interesting features at low temperature: a cubic–tetragonal martensitic transformation in the range $T_M = 40$–50 K, and a superconducting transition at about $T_C = 18$ K [1–3]. The martensitic transition has generated a great deal of interest but it is still not completely understood. Theoretical and experimental results are not conclusive as regards the order of the martensitic anomaly. Early specific heat studies did not give clear evidence about the thermodynamic order of the transition, nor whether there is a correlation between the martensitic and superconducting transition temperatures. In addition, recently specific heat measurements on Nb_3Sn samples in the superconducting state, prepared by solid state diffusion reaction, have been interpreted as showing the presence of an intrinsic second superconducting gap, affecting the electronic density of states [4].

One reason for this lack of understanding of the cubic–tetragonal transformation is that this thermodynamic anomaly was not clearly observed in early heat-pulse calorimetry studies. This may be due to noise in the data [5], too small an anomaly in the total specific heat in ac calorimetry [6], or the absence of the anomaly [4]. It has been inferred, however, that the cubic to tetragonal transformation must be a first-order thermodynamic transition, with a proposed Jahn–Teller mechanism [7, 8] which should be observable as hysteresis in specific heat measurements through the transition, and in entropy measurements. It is very important to mention at this point that a martensitic transition must be necessarily a first-order thermodynamic transition, showing a hysteretic behavior in the specific heat and in resistivity–temperature measurements [9, 10]. In fact for materials displaying this kind of transformation, such as the Al–Cu–Zn alloy, which can be considered as the prototype martensitic alloy [11], a phase transformation is observed from an ordered b.c.c. (β_1) parent phase to an ordered **18R** phase, at different temperatures depending on the composition [9, 11]. In specific heat measurements one can observe the typical hysteresis of the thermodynamic transition at two different temperatures, as well in transport measurements. For the Nb_3Sn case this hysteresis has not been observed with enough precision. Among the reasons for the lack of observation of this anomaly could be non-optimal characteristics of the samples, internal stress, samples with incorrect stoichiometry, compositional inhomogeneity, or inclusive technical deficiencies of the experimental equipment when performing the specific heat measurements [12]. It is important to mention that frequently this A15 alloy presents impurities due to the formation of other

[3] Author to whom any correspondence should be addressed.

compositions and inclusive Sn excess has been often observed. There are two important characteristics of this alloy that must be understood. The first one is related to the debate about the order of the high temperature transition: the so-called martensitic anomaly. The other is related to the influence of the martensitic transition on the electronic density of states, and therefore on the superconducting transition temperature [13]. As regards the first point, Labbe and Friedel [8] in their studies related to the cubic to tetragonal transition proposed that it may involve a Jahn–Teller distortion, occurring in the crystalline structure through the effect of the one-dimensional Nb chains. These chains are among the crystallographic features of the A15 compounds. From this point of view calculations based on electron sub-band models have predicted that the cubic to tetragonal transition is first order. However, experimentally Vieland *et al* [7] presented only indirect evidence that the structural transition is first order (indirect in the sense that the thermodynamic order was inferred from non-thermodynamic measurements), as predicted by theories invoking a band Jahn–Teller distortion. Nevertheless, other experimental results have shown an absence of latent heat and hysteresis at the transition temperature, which has been interpreted as evidence for a thermodynamic transition of the second order [5]. Lastly, we must mention that another physical possibility of the martensitic transformation in this compound could be related to a Peierls distortion, particularly in this case, of the formation of a charge density wave (CDW) promoted by the infinite Nb chains, as was theoretically formulated by Gorkov, Bhatt and McMillan.

The aim of this work is twofold: to clarify the role of the so-called martensitic transition in determining the superconducting temperature, and to prove the possible existence of two superconducting energy gaps, as recently claimed. The results of this investigation can be summarized as follows. Thermodynamic characteristics of seven Nb_3Sn single crystals were determined by means of specific heat measurements. The results show the clear martensitic anomaly around 50 K, and this does not display hysteretic behavior, as expected for a first-order thermodynamic transition, thus suggesting a weak first-order or a second-order transition.

We observe a clear correlation between the superconducting and the so-called martensitic transition temperatures. In addition we observed in the specific heat measurements at low temperatures the existence of a feature related to the presence of only a single energy gap.

In addition, in order to corroborate that our results are obtained for good specimens, we performed x-ray diffraction analysis which shows that the samples are single crystals.

2. Experimental details

The Nb_3Sn samples were grown over a period of four months by means of closed-tube vapor transport with iodine vapor as the transport agent. From the batch of samples we selected seven single-crystalline specimens for our measurements; they consist of just one to several crystals with mm size. Crystallographic characteristics were examined at room temperature by means of x-ray diffraction, using a Siemens P4 diffractometer equipped with Mo Kα radiation ($\lambda = 0.710\,73$ Å).

Electrical resistivity was determined by the four-probe method. These samples were found to have resistivity ratio $R(300\ \mathrm{K})/R(T_C) = 18$ and an extrapolated residual resistivity ratio of $R(300\ \mathrm{K})/R(0\ \mathrm{K}) = 50$, indicating the high degree of purity and crystalline perfection [14]. Early studies with these crystals were performed up to 18 T as reported by Stewart *et al* [15]. As an antecedent of establishing the quality of the crystals, some of the oriented single crystals from this same batch were used for dHvA oscillation studies of the Fermi surface [14]. The crystals were measured and characterized using the magnetization versus temperature, resistance versus temperature, and specific heat versus temperature in order to study the characteristics of the so-called martensitic transformation and the superconducting transition temperature.

Specific heat measurements were performed between room temperature and 2 K under magnetic field below 0.1 Oe, using a thermal relaxation technique with a Quantum Design PPMS calorimeter. Calibrated addenda corrections for the sample holder were subtracted; thus the specific heat measurements show the corrected values for all samples. In the range from 2 to 60 K measurements were taken in multiple cooling and warming cycles.

3. Results and discussion

For the crystallographic characterization we studied two typical samples by means of x-ray diffraction, hereafter called NS1 and NS4, with masses of about 5.31 and 9.5 mg, respectively. X-ray characteristics were taken at a temperature of 298(1) K using a Siemens P4 diffractometer equipped with Mo Kα radiation ($\lambda = 0.710\,73$ Å). Although the samples are large and display somewhat irregular shapes, they were revealed to be single crystals, as reflected by the well defined, symmetric Bragg diffraction peaks; see panel (A) of figure 1—this part of the figure shows the refined data obtained by computing a generated spectrum of the diffraction pattern of the single crystal NS1, whereas panel (B) shows two reflections at two particular positions in the reciprocal space. In this lower panel, ω corresponds to the Bragg angle which according to the diffractometer geometry corresponds to $2\theta/2$. The two reflections, one at low angle $\omega = 9°$, the another at high angle at $\omega = 29.6°$, are representative features for a good single crystal. The reflection peaks at low angles necessarily need to have four characteristics: a single well defined maximum, the peak must be highly symmetric, a ratio of signal to noise that is high, and the same amount of noise to the left and right of the peak. The reflection at $(0, -1, -2)$ presents those characteristics. Whereas the peaks at high angle must have preferentially the higher ratio of signal to noise, they can be non-symmetric because the monochromaticity of the diffraction apparatus needs to be taken into account due to the two contributions of the x-ray diffraction beam ($K\alpha_I + K\alpha_{II}$). Thus, accordingly the ratio of signal to noise is necessarily low due to the fact that the atom scattering factor decreases as the Bragg angle increases. This is intrinsic to any crystal,

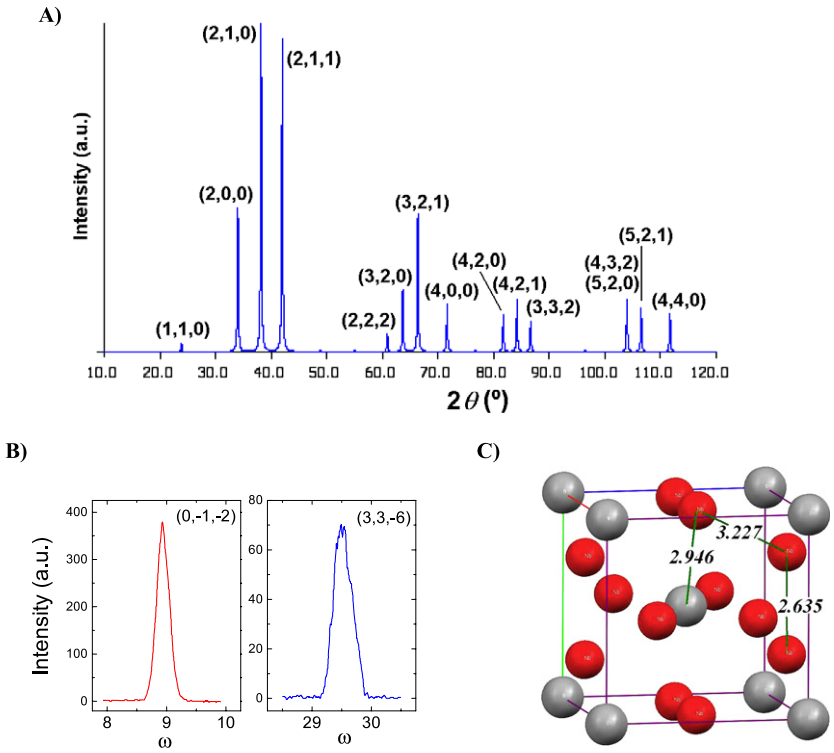

Figure 1. (A) The calculated powder diffraction pattern for Nb_3Sn ($\lambda = 1.5405$ Å, no preferred orientation), computed using x-ray data for the single crystal NS1. Software: CaRine Crystallography (Release 3.1). C Boudias and D Monceau, 1998. (B) Scans for reflections $(0, -1, -2)$ and $(3, 3, -6)$ for crystal NS1 [16]. (C) Crystalline structure of Nb_3Sn. Distances in Å, big spheres in the corners and in the center correspond to Sn and the other spheres to Nb.

good or with low quality. For the NS1 crystal, the reflection at $(3, 3, -6)$ shows clearly that the peak is well defined, and the noise is constant at the two ends of the peak, this meaning that the crystal presents an ideal crystallinity. In addition, we remark that no secondary diffraction patterns were observed, for possible impurities or diffuse scattering. For each sample, a complete diffraction sphere was collected [16] at the highest available resolution (0.62 Å, $2\theta_{max} = 70°$). As expected, the crystals belong to space group $Pm\bar{3}n$ and the structure of Nb_3Sn is an A15-type arrangement, as previously described [12]. Atomic positions were refined [17] on the basis of absorption-corrected data [18]. A characteristic parameter for a crystal is the high value of the extinction coefficient, which converges to identical values for both samples; in these crystals we found 0.82(18) for NS1 and 0.8(2) for NS4 [17]. Assuming that the applied correction covers mixed primary and secondary extinctions, this result suggests that samples should have similar block sizes and similar concentrations of randomly distributed dislocations [19].

In table 1 we present many of the characteristics of the two specimens measured. Both samples are characterized by rather short unit cell parameters, $a = 5.2700(9)$ and $a = 5.2531(13)$ Å, for NS1 and NS4, respectively, while the accepted value found in the literature for crystalline Nb_3Sn is $a = 5.29$ Å [20]. Interestingly, NS1 and NS4 have significantly different cell parameters, and, as a consequence, the cell volume is reduced by about 1% in NS4 compared to NS1. Calculated densities present the same 1% drop. However, using diffraction data, a confident interpretation of such a cell contraction in terms of intrinsic vacancies in the alloy cannot be carried out, at least if departures from Nb_3Sn stoichiometry remain small. In contrast, the high resolution of the diffraction data allows us to accurately determine distances in the solid (table 1). The shortest Nb $\cdots$ Nb separation is reduced from 2.6350(5) Å in NS1 to 2.6266(6) Å in NS4. In the same way, the Nb $\cdots$ Sn separations in NS1 and NS4 are 2.9460(5) and 2.9366(7) Å, respectively.

The two samples examined using x-rays included in this work, NS1 and NS4, have two different characteristics in the high temperature anomaly; see figure 2. Whereas NS1 has a very well defined sharp peak at the specific heat characteristic, which is starting at about 50 K, NS4 presents only a small feature starting at about 46 K. A possible interpretation of the sharpness for these two anomalies may be related to the crystalline structure; if Nb vacancies are present in the structure, then the cell parameters and volume will be reduced, as observed for samples NS1 and NS4. We may speculate that the implication of this behavior might be related to a Peierls distortion in the Nb chains [21, 22]. Thus, the charge density wave (CDW) created due to the distortion will open an energy gap in the direction of the chains, and possibly be better formed if the chains are without Nb vacancies than if there exist deficiencies or vacancies. Therefore, this will reduce the size and sharpness of the anomaly.

We also cannot disregard another possibility; this may be due to the crystal inhomogeneities. As crystals start to grow, it is not surprising to observe sample to sample variations in the A15 structure, albeit differences comparing NS1 and NS4

Table 1. Crystallographic data for two single crystals, NS1 and NS4.

Compound	NS1 (5.31 mg)	NS4 (9.5 mg)
Empirical formula	Nb_3Sn	Nb_3Sn
Formula weight	397.42	397.42
Color, habit	Metallic, irregular	Metallic, prism
Crystal size (mm)	$0.3 \times 0.2 \times 0.2$	$0.4 \times 0.4 \times 0.4$
Space group	$Pm\bar{3}n$	$Pm\bar{3}n$
a (Å)	5.2700(9)	5.2531(13)
V (Å^3)	146.36(4)	144.96(6)
Z	2	2
ρ_{calcd} (g cm^{-3})	9.018	9.105
μ (mm^{-1})	19.54	19.73
2θ range (deg)	11–70	11–70
Reflections collected	2147	1958
$\langle I/\sigma(I)\rangle$	53	109
Independent reflections (R_{int})	72 (0.1978)	69 (0.1953)
Completeness (%)	97.2	95.8
Transmission factors (min, max)	0.015, 0.348	0.014, 0.347
Final R indices (all data) R_1, wR_2	0.054, 0.105	0.062, 0.167
Goodness-of-fit on F^2	1.399	1.309
Extinction coefficient	0.82(18)	0.8(2)
Data/restraints/parameters	72/0/5	69/0/5
Largest difference peak/hole (e Å^{-3})	4.369, −1.789	4.238, −2.807
Final geometric parameters		
Distance		
Nb–Sn (Å)	2.9460 (5)	2.9366 (7)
Nb–Nb (Å)	2.6350 (5)	2.6266 (6)
Nb $\cdots$ Nb (Å)	3.2272 (5)	3.2169 (8)

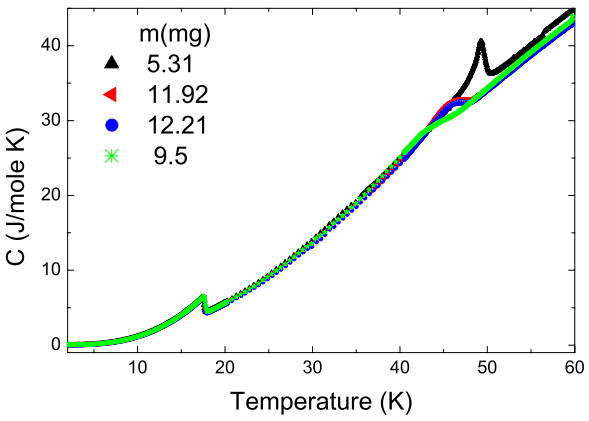

Figure 2. Specific heat versus temperature of four Nb_3Sn single crystals measured between 2 and 60 K. Clearly we observe both transitions. The high temperature transition shows the martensitic anomaly in four samples, the anomalies in the samples presenting different shapes and sizes; no extra anomaly was observed below the superconducting transition.

samples which are considered small. As NS4 is a crystal with a bulk volume about double that of NS1, inhomogeneities may be seen as a natural consequence. However in our set of samples with the slow growing process performed over a period of four months, the inhomogeneities may be very small and our first speculation related to CDW nesting cannot be disregarded. Final important evidence of the perfection of these crystals is provided by studies on the same batch of samples by Arko *et al* [14] related to the Fermi surface with experiments on the de Haas–van Alphen effect, which agree very well with theoretical studies. In the de Haas–van Alphen experiments an important and necessary aspect is related to the inhomogeneities of the crystal structure under study. Those inhomogeneities must be as small as possible in order to observe features of the Fermi surface.

3.1. Specific heat measurements

The specific heat measurements were performed as was explained before. In figure 2 we show data of four Nb_3Sn samples measured in the interval from 2 to 60 K. An interesting characteristic in those measurements is the notably different shapes and temperatures of the high temperature anomaly in the specimens—whereas the superconducting transition temperature at about 18 K presents only a small variation in size and temperature.

Figure 3 depicts the specific heat of the four samples of Nb_3Sn crystals; the martensitic anomaly (T_M) occurs in the interval from 42 to 53 K, and the martensitic anomaly presents different sizes. In this plot the curves were measured in cooling and warming cycles, and there are no hystereses at all; this suggests a weak first-order or second-order thermodynamic transition. Some of these curves display a much clearer anomaly at T_M than has been observed before [5, 6]. In figure 4 the superconducting transitions of the same samples of figure 3 are displayed. The superconducting transition temperature onsets show a small but discernible difference between the four samples, with the high onset for the 9.5 mg sample and

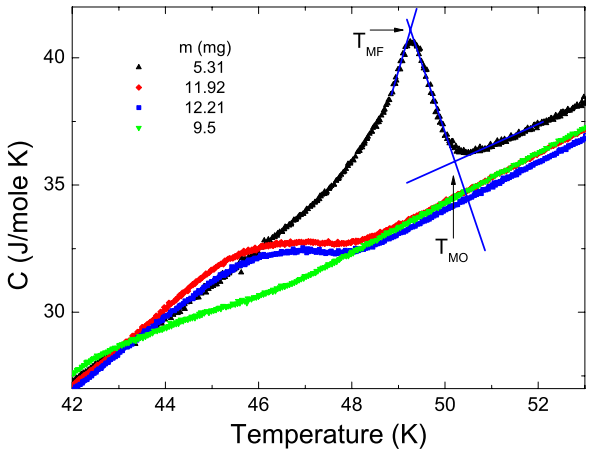

Figure 3. The specific heat versus temperature for four Nb_3Sn single crystals between 42 and 53 K with warming and cooling cycles. Note that there is no observable hysteresis around the martensitic transition. The straight line in one of the curves is presented to show the form for performing the determination of the transition onsets and final temperatures.

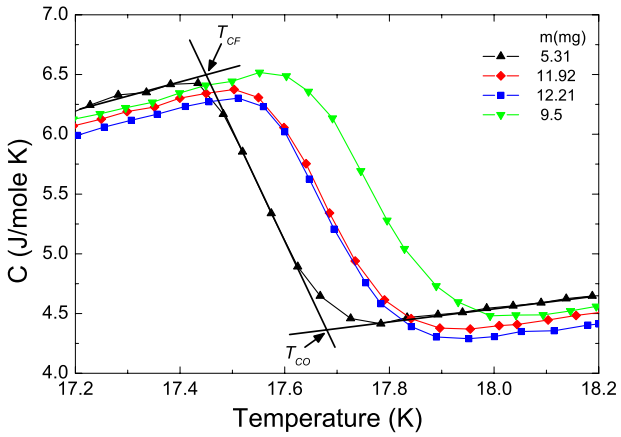

Figure 4. Specific heat versus temperature for the four samples shown in figure 2 around the superconducting transition temperature. The straight lines show the form for determining the transition onsets and final temperatures.

the minimum for the 5.31 mg sample. The approach that we used for the determination of the transition temperatures—onset and final—is also shown in figure 4. There the straight line intersections indicate the transition temperatures.

In figures 3 and 4 there can be observed slight but discernible differences in the onsets of the superconducting transition temperatures, and in the sizes and widths of the martensitic transitions. Note that there is a trend, outside of experimental error, between the two transitions: the superconducting temperature onset decreases as the martensitic temperature onset increases. The differences between samples could arise independently from different amounts of strain or slight differences in composition, or from an intrinsic physical property difference between the two transitions, as mentioned before. The total variation of T_C is small, but quite measurable; however the total variation of T_M is large. It is perhaps not surprising that T_C displays such a small variation among the

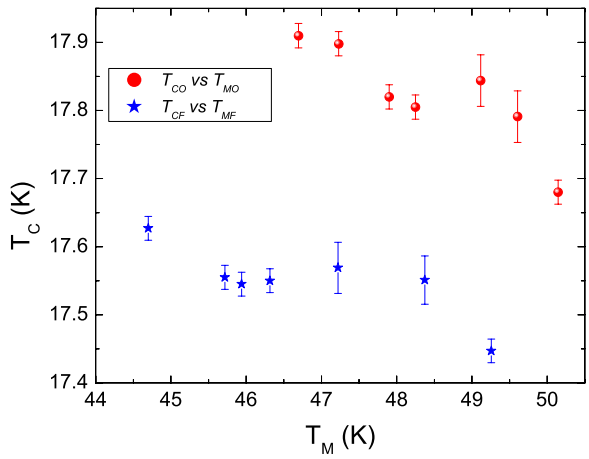

Figure 5. Plots for the transition temperatures; onsets, T_{CO} and T_{MO}, and final ones, T_{CF} and T_{MF}, for both transitions and seven Nb_3Sn crystal samples.

seven crystals since they were taken from the same batch and experienced very similar growth conditions. For the same reason, however, it is surprising that T_M displays such a large variation, namely ten times the T_C change. In figure 5 we show the superconducting transition temperature as a function of the martensitic transition temperature for the seven measurements on the samples. There, we include data for the onset temperatures, superconducting T_{CO} and martensitic T_{MO}, and the superconducting T_{CF} and martensitic T_{MF} temperatures at the end of the transition. A very clear correlation is observed between T_C and T_M. It is important to note in this figure the size of the error bars. In some measurements on some samples, it was quite difficult to distinguish the onsets and final points of the transition temperature in the experimental curves. So in that case the bars are large.

The physical property that could link T_C and T_M is the density of electronic states at the Fermi level. Thus, if the martensitic transition temperature and the size of the peak anomaly decrease, the changes will increase the density of electronic states available for the superconducting transition. This behavior is at least consistent with the idea of a charge density wave (CDW) associated with the martensitic transformation as proposed initially by Gor'kov [21] and continued by Bhatt and McMillan [22] using the Landau theory. This theory presents the possibility of a competition, for the Fermi surface, of the CDW and superconductivity as regards lowering the total energy of the system by opening a CDW energy gap, and therefore using some electron population.

In order to confirm the absence of hysteresis in the specific heat around the martensitic transition in Nb_3Sn, we performed two additional tests: the first one consisted in measuring the specific heat of a single crystal of Cu–Zn–Al, considered by experts in the field as a martensitic prototype alloy that shows a first-order thermodynamic transition. This was previously characterized [9]. The results show hysteresis between the cooling and warming cycles, in agreement with the reported austenite and martensitic temperature values [9]. However, we should mention that the martensitic anomaly in this compound

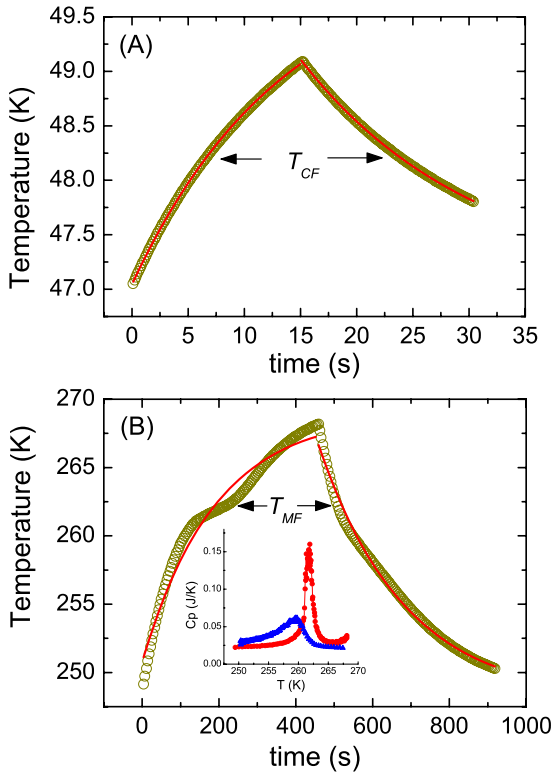

Figure 6. Temperature relaxation time curves in the vicinity of the maximum of the martensitic transition of (A) Nb_3Sn and (B) Cu–Zn–Al. Note that for Cu–Zn–Al there is a distortion, which is a characteristic of a first-order transition. Continuous lines show an exponential decay fitting. The arrows indicate the end of the transition temperatures. The inset of figure (B) presents the specific heat curves in warming and cooling cycles.

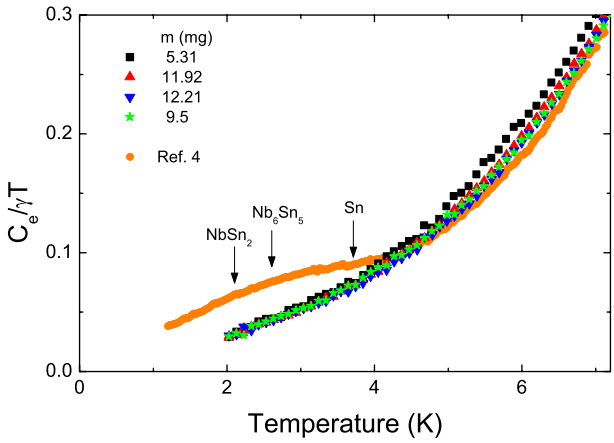

Figure 7. Specific heat measurements for four of our single-crystal specimens of Nb_3Sn at low temperature, and specific heat measurements from the authors of [4]. Note the feature below 4 K that the authors of this reference claim is related to a second energy gap. Our measurements for pure single crystals do not show that anomaly. Arrows indicate the T_C for possible superconductors that may be formed in polycrystalline samples.

does not show a lambda-type transition, as measured with our PPMS. The reason is the algorithm used for the calculation of the specific heat, which is not adequate for a first-order transitions measurement [23]. The second test was to calculate the specific heat from the raw temperature–time data using Bachmann's approach, as suggested by Lashley *et al* [23]. The results obtained with the Cu–Zn–Al sample show a hysteresis and a transition anomaly four times higher than what was observed with the PPMS. The same approach was applied to the Nb_3Sn crystal samples; the results show practically the same curves as were obtained using the PPMS algorithm and with Bachmann's approach—the difference consists in the specific heat determined with Bachmann's approach being noisy.

In figure 6 we show the thermal relaxation data for the Nb_3Sn crystal sample (A) with mass equal to 6.5 mg, and for the Cu–Zn–Al martensitic single crystal, sample (B). This figure illustrates the difference between a first-order and second-order transition. There we indicate with arrows the temperature of the end of the transition, T_{MF}, where the change in the specific heat is most notorious. The continuous line is a fit based on the sum of two exponential decay functions, that involve two relaxation time constants. Note that the fitting reproduces adequately the Nb_3Sn relaxation experimental data. In figure 6(B) we note that the fitting to the experimental relaxation curves does not reproduce the Cu–Zn–Al relaxation experimental data. In the inset of figure 6(B) we present the specific heat curves for the Al–Cu–Al alloy measured in the two cycles: lowering and raising the temperature. A hysteresis is clearly noted. The features are similar to those of early specific heat studies and measurements performed by Tsumura *et al* [9].

Figure 7 shows an interesting comparison of the normalized specific heat for four of our specimens and the Guritanu *et al* early measurements on their polycrystalline sample. This plot is displayed in terms of $C/\gamma T$ versus temperature. At the temperature below 6 K it seems that our samples do not present any anomaly as those of Guritanu *et al* do, that they mention as a feature of a second energy gap. In this figure we included the superconducting transition temperatures of impurities that frequently are found in Nb_3Sn polycrystalline samples (indicated by arrows) as possible contaminants. These common impurities are $NbSn_2$ (T_C = 2.1 K), Nb_6Sn_5 (T_C = 2.6 K) and Sn (T_C = 3.7 K). Note that these impurities have transition temperatures in the temperature range where the C_p reported in [4] presents the anomaly, and which is absent in our measurements.

4. Conclusions

In conclusion, in this work we present new specific heat measurements performed on high quality Nb_3Sn single crystals. Due to the excellent quality of the samples, we have observed a clear specific heat feature at the martensitic transition. In multiple cooling and heating cycles, we did not observe hysteretic behavior in the specific heat measurements as a function of temperature. Our measurements imply that the so-called martensitic transition is a second-order or weakly first-order transition, perhaps related to a charge density wave or Peierls distortion. The samples SN1 and SN4 examined using x-ray diffraction present the specific heat anomaly in

very different forms: whereas SN1 has a very well defined sharp peak, with its onset at about 50 K, SN4 presents only a small feature with its onset at about 46 K. We speculated that this effect is a consequence of vacancies in the Nb chains, and consequently the martensitic anomaly could be related to a Peierls distortion.

This study shows the existence of a correlation between the superconducting transition temperature and the anomaly at high temperature.

At the lowest temperatures, from around 2 to 20 K, we observed only one superconducting energy gap feature. Our data for the specific heat measurements in this temperature interval do not show any feature or anomaly at low temperature that could be related to a second energy gap.

Acknowledgments

We thank R Black from Quantum Design for help with the new software and helpful discussions. RE thanks the support from DGAPA-UNAM. We also thank F Silvar for helium provision and G W Webb from the University of California for kindly providing the samples used in this study.

References

[1] Mailfert R, Batterman B W and Hanak J J 1967 *Phys. Lett.* A **24** 315
[2] Mailfert R, Batterman B W and Hanak J J 1967 *Phys. Status Solidi* **32** K67
[3] Weger M and Goldberg I B 1971 *Solid State Physics* vol 28, ed F Seitz and D Turbull (New York: Academic) p 1
[4] Guritanu V, Goldacker W, Bouquet F, Wang Y, Lortz R, Goll G and Junod A 2004 *Phys. Rev.* B **70** 184526
[5] Vieland L J and Wicklund A W 1969 *Solid State Commun.* **7** 37
[6] Chu C W and Vieland L J 1974 *J. Low Temp. Phys.* **17** 25
[7] Vieland L J, Cohen R W and Rehwald W 1971 *Phys. Rev. Lett.* **26** 373
[8] Labbe J and Friedel J 1966 *J. Physique* **27** 153
Labbe J and Friedel J 1966 *J. Physique* **27** 708
[9] Tsumura R, Rios D, Chaves M, Rodríguez L, Akachi T and Escudero R 1988 *Phys. Status Solidi* a **105** 411
[10] Makita T, Kobukata M and Nagasawa A 1986 *J. Mater. Sci.* **21** 2212
[11] Lovey F C and Torra V 1999 *Prog. Mater. Sci.* **44** 189
[12] Testardi L R 1975 *Rev. Mod. Phys.* **47** 637
[13] Weber W and Mattheiss L F 1982 *Phys. Rev.* B **25** 2270
[14] Arko A J, Lowndes D H, Muller F A, Roeland L W, Wolfrat J, van Kessel A T, Myron H W, Mueller F M and Webb G W 1978 *Phys. Rev. Lett.* **40** 1590
[15] Stewart G R, Cort B and Webb G W 1981 *Phys. Rev* B **24** 3841
[16] 1999 *Siemens XSCANS* Version 2.31 (Madison, WI: Siemens Analytical X-Ray Instruments Inc.)
[17] Sheldrick G M 2008 *Acta Crystallogr.* A **64** 112
[18] Walker N and Stuart D 1983 *Acta Crystallogr.* A **39** 158
[19] Masimov M 2007 *Cryst. Res. Technol.* **42** 562
[20] PDF-19-0875. See also: Maier R G 1969 *Z. Naturf.* a **24** 1033
[21] Gorkov L P 1973 *Zh. Eksp. Teor. Fiz. Pis. Red.* **17** 525
Gorkov L P 1974 *Sov. Phys.—JETP* **38** 830 (Engl. Transl.)
Gorkov L P and Dorokhov O N 1976 *J. Low Temp. Phys.* **22** 1
Gorkov L P and Dorokhov O N 1975 *Zh. Eksp. Teor. Fiz. Pis. Red.* **21** 656
Gorkov L P and Dorokhov O N 1975 *JETP Lett.* **21** 310 (Engl. Transl.)
[22] Bhatt R N and McMillan W L 1976 *Phys. Rev.* B **14** 1007
[23] Lashley J C *et al* 2003 *Cryogenics* **43** 369